ISSN 1062-7391, Journal of Mining Science, 2020, Vol. 56, No. 6, pp. 1024–1031. © Pleiades Publishing, Ltd., 2020.
Russian Text © The Author(s), 2020, published in Fiziko-Tekhnicheskie Problemy Razrabotki Poleznykh Iskopaemykh, 2020, No. 6, pp. 161–169.

MINE AEROGASDYNAMICS

Optimizing Design of Blades for High-Speed Axial Fans

A. M. Krasyuk[a]* and E. Yu. Russky[a]

[a]*Chinakal Institute of Mining, Siberian Branch, Russian Academy of Sciences, Novosibirsk, 630091 Russia*

**e-mail: krasuk@cn.ru*

Received July 13, 2020
Revised September 21, 2020
Accepted November 3, 2020

Abstract—The mathematical methods of structural design optimization using the optimality criteria are reviewed. The resultant and nearly optimal design of a fan bade ensures the design goals at the selected criterion. The optimal design based on topology optimization was carried out in ANSYS. The optimization problem solution provided optimal distribution of the impeller blade mass for axial mine fans. It is validated to be possible to decrease the the blade mass by 60% as compared with a monolithic blade at the preserved rotation speed and ratio of flow path diameters.

Keywords: Blade, axial fan, ANSYS, optimality, strength, design variables, stress.

DOI: 10.1134/S1062739120060149

INTRODUCTION

Safety of underground mining depends on the efficiency of mine ventilation and its master link represented by main fans. Design and engineering of high-end main mine fans is yet a critical objective. The most efficient way of enhancing the main mine fan capacity is increasing the circumferencial speed of fan blades. Commonly used in mines in Russia, axial two-stage fans (series VOD), have tip speed of blades at 78.5 m/s. The ultimate tip speed of blades of the most main mine fans manufactured in Russia is no higher than 105–120 m/s. This is conditioned by high value of normal inertia of blades and by strength of the blade materials. In case of higher velocity, it is required to ensure the strength of the blades and impeller. The tip speeds of blades above 150–160 m/s dictate reduced normal inertia and, consequently, lower weight of the blades.

With a view to decreasing the weight of blades at the preset loads, it is possible to select materials having lower density and higher strength, or to optimize structural topology of the blades [1, 2]. Earlier, the Institute of Mining, SB RAS has succeeded in reduction of the blade weight by designing a cellular structure of the core [1, 2]: the cellular structure core with working and auxiliary surfaces (plates) as in Fig. 1. As a consequence, the weight of AK7 aluminium alloy blades [3] was reduced by 51%, the tip speed of the blades was increased to 140 m/s and the capacity of mine fans was enhanced by 1.5–1.7 times. The weight reduction became possible thanks to topological optimization of core material.

This study objective is optimization of design values of axial fan blades in order to reduce their weight and, thus, to increase their rotational speeds up to 230 m/s at the stresses and strains maintained within permissible ranges (effective stresses should never exceed critical stresses).

(a) (b)

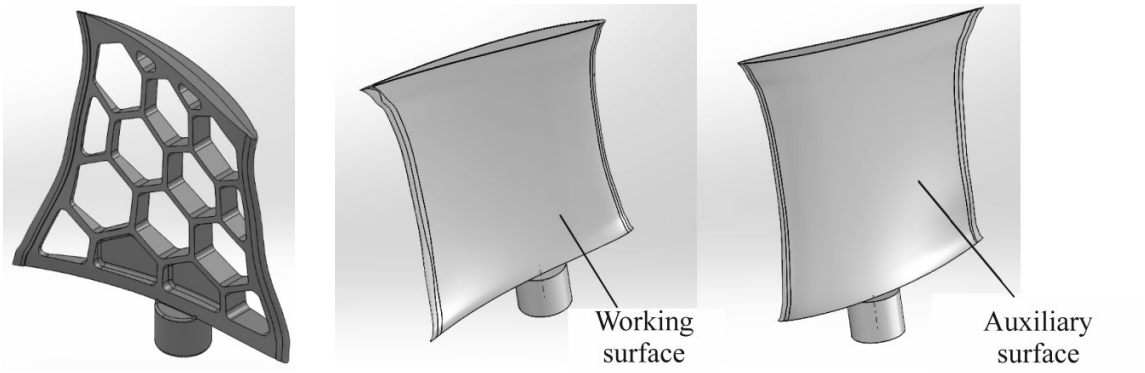

Fig. 1. General view of (a) axial fan blade and (b) cellular structure core.

1. TOPOLOGICAL OPTIMIZATION

Topological optimization widely uses such methods as SIMP (Solid Isotropic Material with Penalty) ESO (Evolutionary Structural Optimization), Level-Set method and various combinations of these techniques [4–7]. We use SIMP implemented in ANSYS. The material structure is assigned a certain density from 0 to 1, which is interpreted as dependence of the material porosity on the stresses in different areas of the structure. The stiffness and density of the material observe the power law given by [4]:

$$E_{ijkl}(x) = \rho(x) p E_{0ijkl} .$$

Here, $E_{ijkl}(x)$ and E_{0ijkl} are the current and initial tensors of elasticity of the material, respectively (i, j, k, $l = 1, 2, 3$); $\rho(x)$ is the function of density, x is the current iterating step; p is the penalty factor, $p > 1$ [8, 9]. The penalty size is usually selected in the known range [5].

The density function is the dependence of the initial density on the current iteration: $\rho(x) = x\rho_0$ (ρ_0 is the initial density of material, x is the current step of iterative process). In the iterative process, the finite elements with the density less than the pre-set value are withdrawn by means of nullification of the suitable stiffness matrix of the element. The blade design optimization uses the finite element method [10, 11] implemented in ANSYS, with topological optimization based on the evolutionary stress–strain analysis. The topological optimization means optimized distribution of material in a pre-set volume at the pre-set loads and boundary conditions. The design domain is the inner volume of the blade, while the external aerodynamic (working and auxiliary) surfaces are fixed (Fig. 1b).

The objective function is the minimal yield (maximal stiffness) of the blade design, determined from the preliminary static calculation. The optimality criterion is the blade weight changed by means of varying the inner volume of the blade between the working and auxiliary surfaces (Fig. 1b). The optimization parameter is the function of material distribution in the inner volume inside the unchangeable external boundaries while the changes take place inside the inner volume. The design constraints are the weight, maximal stresses and fixturing conditions.

Efficient optimization can allow the high-capacity fan blades to be manufactured from AK7 aluminium alloy to operate at high rotation speeds and at high efficiency. As a consequence, it can be possible to reduce the specific area of the main fan construction ($k = Q / S$, Q is the fan capacity, m^3/s; S is the fan construction site area, m^2), to decrease the size of safety pillars under the main fan building, as well as to upgrade old ventilation installations owing to replacement of the rotors for the fans of the same size but with much higher rotational speed and efficiency.

2. OPTIMIZATION OF VOD-40 FAN BLADE

Fan blade design optimization is discussed as a case-study of mine fan installation operating in a Kuzbass mine, with impeller diameter of 400 mm. The mine modernization projects involves ventilation at the fan operating conditions as $Q = 500$ m^3/s and $P_{SV} = 2000$ Pa. The fan installation is composed of VOD-40 fans with exhausted operational life, which can ensure maximum air flow rate of 350 m^3/s at $P_{SV} = 2000$ Pa. It is impossible to equip the fan installation with larger diameter fans as the mine yard is small. The fan modernization means improved aerodynamic performance at the same diameter impeller at the higher rotation speed. As the loads on blades are increased due to higher rotation speed and, consequently, higher normal inertia (centrifugal forces), the existing blades have insufficient strength.

In order to reduce centrifugal forces by making the blade lighter, the blade is made as a composite structure: an optimized shape cast core with welded curved plates making the working and auxiliary surfaces of the blade (Fig. 1b) manufactured form AK7 aluminium alloy (elasticity modulus of 69 Pa, Poison's ratio $\mu = 0.27$, ultimate stress limit $\sigma_{\text{lim}} = 185 - 485$ MPa as per setting, yield point $\sigma_y = 95 - 415$ MPa as per setting).

It is assumed that the yield point $\sigma_y = 324$ MPa, safety factor $n = 1.8$ and permissible stress $\sigma_{perm} = \sigma_y / n = 180$ MPa. The stem is dead fixed. The optimization constraints include: minimal maximum von Mises stress of 180 MPa (with regard to safety factor of 1.8) and the weight is not less than 30% of the initial weight. Using these criteria, the core design is selected (internal geometry of the blade) as the optimized structure at the preset loads and grip conditions. This optimized structure is assumed as the preliminary conceptual 3D model for the interpretation of a FEM-based model before passing to a solid model. The optimization-based solid modeling using a set of separate components, and the operation of the solid model are sufficiently complex processes. The shape of the optimized blade should be finalized with regard to its manufacturability, manufacture cost and some other factors. A disadvantage of the parametric optimization is the possible change in the strength characteristics under smoothing and conversion of the FEM model to a solid model. Figure 2 depicts convergence of the iterative processes (30–40 iterations in the problem under discussion).

The axial fans have a ratio between the sleeve diameter d and the internal diameter of the fan body D: $v = d/D = 0.5$–0.6. Table 1 presents the blade design optimization results at $v = 0.5$ and $v = 0.6$ and at various optimization constraints. At $v = 0.6$ the blade weight $m = 78.0$ kg; at $v = 0.5$ $m = 96.1$ kg (the blade is longer). For $v = 0.6$ of the initial (solid) blade, the stresses are under the permissible value of 180 MPa at the tip speed not higher than 167.5 m/s. The same stress level hold true for the blade with the optimized core when the blade weight makes 40% of the solid blade weight. At higher tip speed, permissible stresses are only ensured in case of the optimized structure blades.

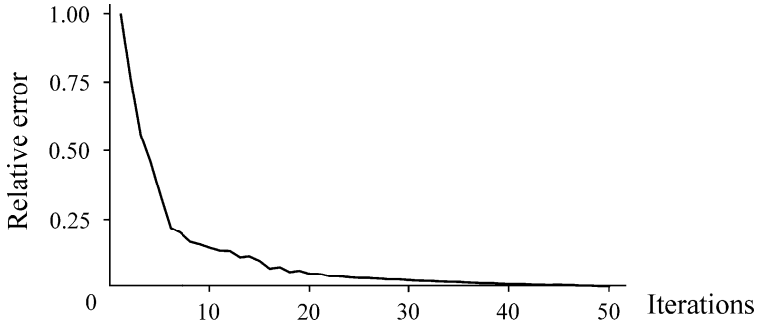

Fig. 2. Convergence of iterative process.

Table 1. Blade optimization results

Rotational speed of impeller, rpm / tip speed of blades, m/s	Blade weight, kg		Stresses, MPa / displacements in blades before optimization, m
	at weight constraint	at maximal stress constraint	
$\nu = 0.6$			
1200 / 251.3	29.84	38.44	406.0 / 0.001970
1000 / 209.4	30.09	40.59	282.0 / 0.001370
800 / 167.5	26.12	35.20	180.0 / 0.000876
600 / 125.6	22.12	37.36	101.6 / 0.000492
400 / 86.8	21.93	36.46	45.1 / 0.000219
$\nu = 0.5$			
1200 / 251.3	39.19	53.75	224.4 / 0.00270
1000 / 209.4	39.05	53.08	155.8 / 0.00171
800 / 167.5	39.03	53.52	99.7 / 0.00123
600 / 125.6	39.08	52.79	56.1 / 0.00069
400 / 86.8	39.24	52.71	24.9 / 0.00027

The common pattern of the material distribution in the blade structure under the action of centrifugal forces is as follows: at the maximal stress constraint—two fan-out branches (Figs. 3a and 3b); at the weight constraint—one branch with a fork in the periphery (Fig. 4b).

The structure of the optimized blade core experiences the influence of the blade weight and the weight distribution along the blade length: in case of a longer and narrower blade (sleeve ration of 0.5 and less), the foot is less heavier than in a wider blade of the same length. For blades with the sleeve ratio of 0.6, the foot is heavy, with short and extensional branches. The blade structure may differ depending on the optimization constraints: at для $\nu = 0.6$ and at the weight and maximal stress constraints, the structure has a heavy foot and two branches (Figs. 3a and 3b); at $\nu = 0.5$ and at the weight constraints, there is a heavy foot and two branches, too (Fig. 4a) while at the maximal stress constraint, there is a heavy foot and one branch (Fig. 4b).

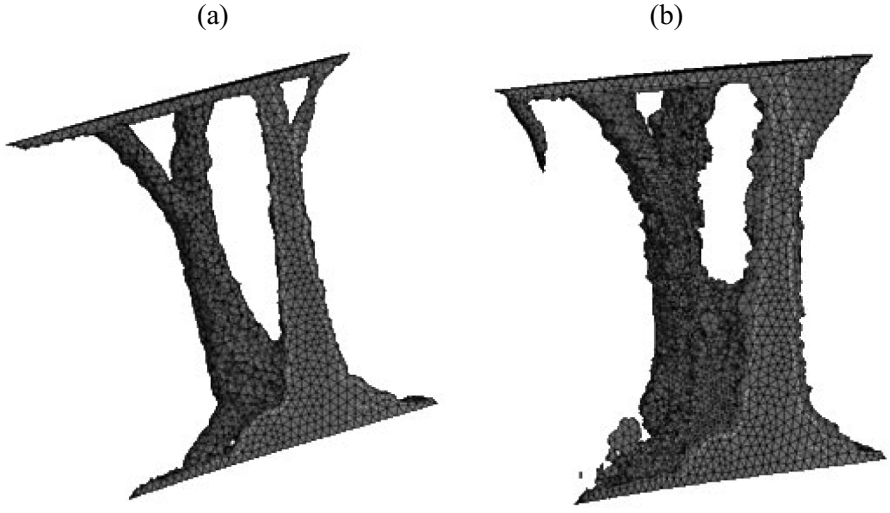

Fig. 3. Material distribution in blade core at $\nu = 0.6$ after optimization: (a) 400 rpm; (b) 1000 rpm.

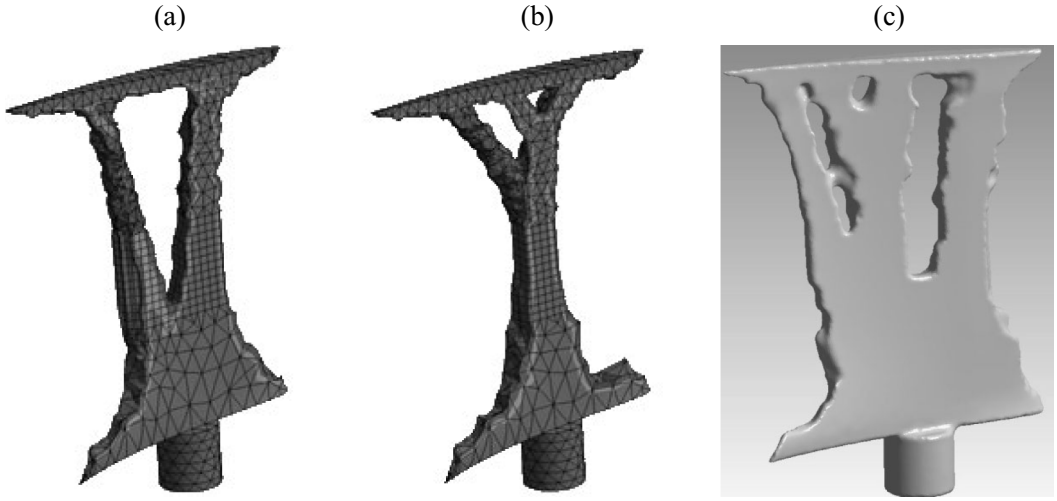

Fig. 4. Material distribution in blade core (1000 rpm, $\nu = 0.5$) after optimization at (a) maximal stress constraint and (b) weight constraint. (c) Smoother model of blade core (1000 rpm, $\nu = 0.6$).

3. VERIFICATION OF STRENGTH OPTIMIZATION RESULTS

For the checking calculation of strength in case of the optimized blade geometry, the obtained model is converted to solid geometry, and the final calculation model has a different shape. The differences can be insignificant (e.g. smoothing of the geometry), or significant (correction of voids, uncoupled geometrical elements, etc.). Optimization should always be verified by means of the checking calculation of strength.

Figure 4c shows the blade model after mesh smoothing and preparation for the checking calculation of strength. The weight of the smoothed model is 74.8 kg, which is 10.5% more than the weight of the blade without smoothing (67.7 kg, blade weight before optimization is 96.1 kg). The optimized distribution of the material in the blade volume (Figs. 3 and 4) is independent of the material density; i.e., for the aluminium alloy with the density of 2700 kg/m^3 and steel with the density of 7850 kg/m^3, the structure represented by the heavy foot and two fan-out branches remains unchanged. The optimized blade weight (21.9–30.1 kg) is comparable with the weight of the blade of a tree structure (45 кг) examined in [1] at the same level of stresses. The explanation is that the tree structure is almost an optimum.

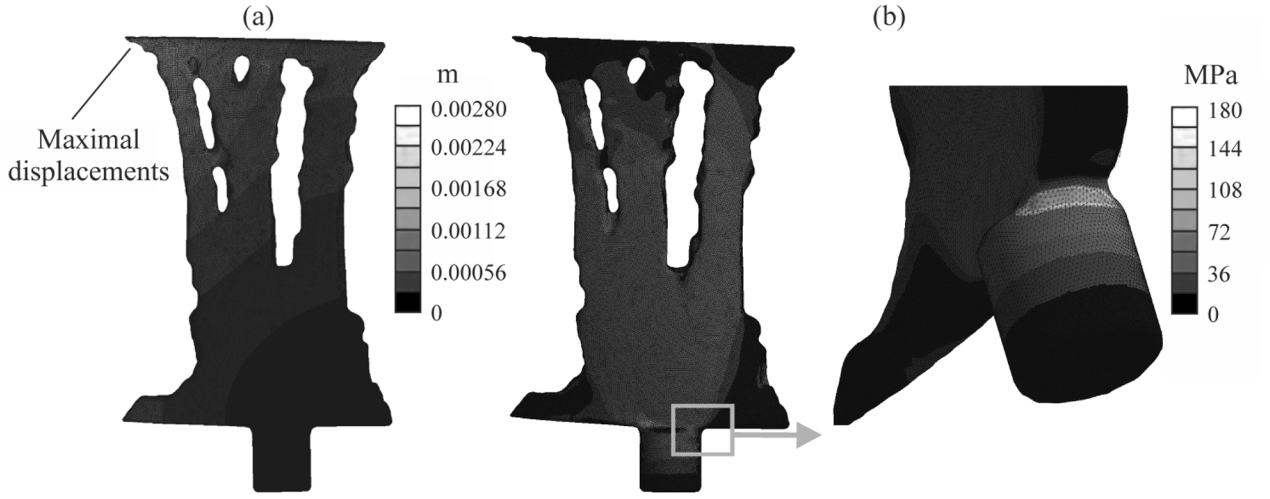

Fig. 5. (a) Displacements in the core and (b) von Mises stresses in the core and stem of the blade after checking calculation at 1000 rpm, $\nu = 0.6$.

Figure depicts the checking calculation aimed at the stress–strain analysis of the blade core and stem after optimization. It follows from Fig. 5b, the maximal stresses are 180 MPa, which agrees with the permissible stresses at the safety factor $n = 1.8$ given by $n = \sigma_y / \sigma_{\max}$ (σ_y is the yield stress, $\sigma_{\max}$ is the maximal stress in the structure).

4. FREE AND FORCED OSCILLATIONS IN THE BLADE

The free and forces oscillations are analyzed in the optimized structure and solid structure blades. Resonances appear in blades when the frequencies of free oscillations of blades become equal or multiple by rotary speed $(f = kn_c)$. The multiplicity k is determined based on the machine layout. Rotor unbalance can induce oscillations in blades at a frequency equal to rotary speed per second, at $k = 1$ [12]. Hazardous modes can appear in axial fans due to vibrations of the blades under the action of transient aerodynamic forces which are induced because of nonuniform flow in interaction between guide apparatus ribbing and straightener blades. In this case, the multiplicities are proportional to the number of guide apparatus ribs, N_P, and in reverse, to the number of straightener blades, N_{CA}. The oscillations can be induced by stalling flutter, which is self-exciting oscillations of blades under interference of aerodynamic forces and elastic forces of blades. When flow energy is sufficient to maintain the process, the oscillations become sustained. The stalling flatter can be caused by the stall in flow through blades at high angle of incidence. Stalls are observed not at all blades but on a group of blade, and the stalling zone can move along the circumference. This phenomenon is called rotating stall. For such oscillations, frequency depends on the number of the stall zones in the rotational flow, N_{BO}, and in general case is aliquant by the rotary speed of impeller. The resonance frequencies in case of the two latter types of oscillations can be given by [13–15]:

$$\omega_n^P = nN_P\omega, \quad \omega_n^{CA} = nN_{CA}\omega, \quad \omega_n^{BO} = nN_{BO}(1-\alpha)\omega,$$

where $n = 1, 2, 3, \ldots$ is the number of harmonic of the exciting forces; $0 < \alpha < 1$.

For VOD-40 fan, at the rotational speed of the fan impeller $\omega = 104.70$ s^{-1} (1000 rpm), number of the guide vane ribs, $N_P = 12$, number of the straightener blades, $N_{CA} = 15$, and the number of stall zones in rotational flow, $N_{BO} = 2$–4, the frequencies of the exciting forces generated by the guide vane ribbing, straightener blades and rotating stall are given by:

$$\omega_n^P = 12n\omega \text{ s}^{-1}, \quad \omega_n^{CA} = 15n\omega \text{ s}^{-1}, \quad \omega_n^{BO} = 4n\omega \text{ s}^{-1},$$

$$\text{or} \quad \omega_n^P = 1256.4n \text{ s}^{-1}, \quad \omega_n^{CA} = 1570.5n \text{ s}^{-1}, \quad \omega_n^{BO} \le 418.8n \text{ s}^{-1}.$$

Table 2 compiles calculations of frequencies of free oscillations in solid and optimized blades, as well as frequencies of exciting forces. The free frequencies in the optimized blades are much higher (up to 4 times) than in the cast solid blades. Furthermore, the exciting frequencies can exceed the free frequencies up to 8.7 times, which eliminates any resonance phenomena.

Table 2. Frequencies in blades at sleeve ratio $v = 0.6$

Number of harmonic	Free frequency, Hz		Exciting frequency		
	Solid blade	Optimized blade	ω_n^P	ω_n^{CA}	ω_n^{BO}
1	61.68	252.03	1256.4	1570.5	418.8
2	160.52	295.53	2512.8	3141.0	837.6
3	207.99	576.85	3769.2	4711.5	1256.4
4	322.32	671.25	5025.6	6282.0	1675.2
5	465.77	720.20	6282.0	7852.5	2094.0

CONCLUSIONS

Topological optimization has enabled the optimized distribution of material in the core of a blade of the axial mine fan impeller, at the essential reduction in the blade weight under the same stresses and strains experience by the structure within the permissible range of the rotation speeds and sleeve ratios. The weight of the blade is reduced by 50–70% as compared with the solid blade. For the fan with the impeller diameter of 4.0 m and sleeve ratio $\nu = 0.6$, the blade weight after optimization is 36.3 kg (at the boundary conditions represented by the maximal von Mises stresses) and 23.5 kg (at the boundary conditions represented by the minimal weight of the blade). The free oscillation frequencies of the blade after its weight optimization are much higher (up to 4 times) than in the cast solid blade. The exciting frequencies can exceed the free frequencies up to 8.7 times, which eliminates any resonance phenomena. The obtained results enable designing fan blades capable to preserve strength at the tip speeds of blades up to 230 m/s.

FUNDING

The study was carried out within the framework of the Federal Research Program, project no. AAAA-A17-117091320027-5.

REFERENCES

1. Krasyuk, A., Russky, E., Lugin, I., and Popov, N., Engineering and Analysis of Aerodynamics and Design Parameters for Metro Tunnel Fans with the Same Blade for Different Core/Tip Diameter Ratios, *Proc. of IFOST-2016, 11th Int. Forum on Strategic Technol*., 2016, pp. 594–598.
2. Ai, Z., Qin, G., Lin, J., Chen, X., and He, W., Variable-Speed Method for Improving the Performance of a Mine Counter-Rotating Fan, *Energy Sci. and Eng*., 2020, vol. 8, no. 7, pp. 2412–2425.
3. RF State Standard, *GOST 1583-93*.
4. Eschenauer, H. and Olhoff, N., Topology Optimization of Continuum Structures: A Review, *ASME Applied Mech. Rev*., 2001, vol. 54, no. 4, pp. 331–390.
5. Zhao, J., Du, F., and Yao, W., Structural Analysis and Topology Optimization of a Bent-Bar-Frame Piston Based on the Variable Density Approach, *Proc. of the ASME 2014 Dynamic Systems and Control Conf*., 2014, pp. 1–7.
6. Du, F. and Tao, Z., Study on Lightweight of the Engine Piston Based on Topology Optimization, *Adv. Materials Res*., 2011, vol. 201–203, pp. 1308–1311.
7. Barbieria, S.G., Giacopinia, M., Mangerugaa, V., and Mantovani, S.A., Design Strategy Based on Topology Optimization Techniques for an Additive Manufactured High Performance Engine Piston, *Proc. Manufacturing*, 2017, vol. 11, pp. 641–649.
8. Hu, J., Li, M., Yang, X., and Gao, S.,Cellular Structure Design Based on Free Material Optimization under Connectivity Control, *CAD Comp. Aided Design*, 2020, vol. 127, 102854.
9. Zhao, L.A., Xu, B.A., Han, Y.A., and Rong, J.B., Continuum Structural Topological Optimization with Dynamic Stress Response Constraints, *Adv. in Eng. Software*, 2020, vol. 148, 102834.
10. Zienkiewicz, O.C., *The Finite Element Method in Engineering Science*, 2nd Edition, McGraw Hill, 1971.

11. Bazhenov, V.A., *Chislennye metody v mekhanike* (Numerical Methods in Mechanical Science), Moscow: Vyssh. shk., 2005.
12. Yang, Y.A., Ouyang, H.B., Yang, Y.A., Cao, D.C., and Wang, K., Vibration Analysis of a Dual-Rotor-Bearing-Double Casing System with Pedestal Looseness and Multi-Stage Turbine Blade-Casing Rub, *Mech. Systems and Signal Proc*., 2020, vol. 143, 106845.
13. Krasyuk, A.M., Lugin, I.V., Russky, E.Yu., and Popov, N.A., Substantiation of Parameters and Estimation of Strength for Basic Structural Units of Axial Tunnel Fan, *Journal of Mining Science*, 2015, vol. 51, pp. 1139–1149. Available at: https://doi.org/10.1134/S1062739115060415.
14. Krasyuk, A.M., Lugin, I.V., Russky, E.Yu., and Kosykh, P.V., Substantiation of Life Extension Method for Two-Stage Axial Flow Fans for Main Ventilation, *Journal of Mining Science*, 2019, vol. 55, pp. 478–493. Available at: https://doi.org/10.1134/S1062739119035818.
15. Hron, R., Martaus, F., Kadlec, M., and Růžek, R., Experimental Axial Fan with Geopolymer Blades, *Proc. 18th Int. Multidisciplinary Sci. Geoconf*., 2018, vol. 18, no. 6.4, pp. 385–392.